Proceedings of IMECE'03
2003 ASME International Mechanical Engineering Congress
Washington, D.C., November 15–21, 2003

IMECE2003-42540

DEVELOPING VARIATIONAL VIBRATION MODELS OF DAMAGED BEAMS: TOWARD INTELLIGENT FAILURE DETECTION

Daniel A. McAdams*
David Comella
Department of Mechanical and Aerospace Engineering
and Engineering Mechanics
University of Missouri-Rolla
Rolla, Missouri 65409-0050
Phone: 573-341-4494
Email: dmcadams@umr.edu

Irem Y. Tumer
Computational Sciences Division, MS 269-3
NASA Ames Research Center
Moffett Field, CA 94035-1000
Phone: 650-604-2976
Email: itumer@mail.arc.nasa.gov

ABSTRACT

Inaccuracies in the modeling assumptions about the distributional characteristics of the monitored signatures have been shown to cause frequent false positives in vehicle monitoring systems for high-risk aerospace applications. To enable the development of robust fault detection methods, this work explores the deterministic as well as variational characteristics of failure signatures. Specifically, we explore the combined impact of crack damage and manufacturing variation on the vibrational characteristics of beams. The transverse vibration and associated eigenfrequencies of the beams are considered. Two different approaches are used to model beam vibrations with and without crack damage. The first aproach uses separation of variables. This method enables the direct integration of the resulting ordinary differential equation and determination of different eigenfrequencies and eigenmodes. This approach uses a spring to model localized reduction in stiffness as a result of the cracked beam. The second approach uses a finite difference approach to enable the inclusion of both cracks and manufacturing variation to be considered. The crack model used with the finite difference approach is based on a localized decrease in the Young's modulus. Using both beam and crack models, Monte Carlo simulations are used to explore the impacts of manufacturing variation on damaged and undamaged beams. Derivations are presented for both models. Conclusions are presented on the choice of modeling techniques to define crack damage, and its impact on the monitored signal, followed by conclusions about the distributional characteristics of the monitored signatures when exposed to random manufacturing variations.

NOMENCLATURE

a	crack depth
b	width of beam
c	local compliance of damaged beam
d	damage parameter
$f(x,t)$	external force applied to a beam
dim	dimension with random variation
dim_n	nominal dimension value
h	height of a beam's cross section
i	integer multiplier for axial location
j	integer multiplier for time
n	denotes the left end of the beam
p	eiegenfrequency of beam
$rand$	random number between zero and one
t	time
w	lateral deflection of beam as a function of space and time
$w_0(x)$	initial deflection of the beam
x	horizontal coordinate

* Address all correspondence to this author.

A	cross sectional area of beam cross section
A_d	area of a beam's cross section affected by damage
A_t	total area of a beam's cross section
E	Young's modulus of elasticity
E_o	undamaged or ideal Young's modulus of elasticity
EI	flexural stiffness of a beam
I	area moment of inertia
L	Length of beam
K	stress intensity factor
β	non-dimensional horizontal crack location
λ	ratio of crack depth to beam height
ν	Poisson's ratio
ρ	density
ρA	mass per unit length of a beam
Δt	uniform time step size
Δx	uniform axial step size

INTRODUCTION

Background and Motivation

Even though failures in complex vehicle systems for NASA applications are *rare* events, the occurrence of such failures is unacceptable at any rate, resulting in a serious need to understand the true characteristics of such events. The rarity of this failure information in such high-risk applications makes it quite challenging to model the typical "expected" response (required for models used in vehicle health monitoring systems) and match this response with empirical data (from which decisions are made.) The inability to match the expected characteristics with empirical observations plays a major role in the unreliability of vehicle monitoring systems, which typically suffer from high rates of false alarms and missed detections.

In the actual operating environment, aerospace systems exhibit significant variability [1, 2]. For example, research in analyzing actual flight data has revealed several sources of variation that are not incorporated into conventional aircraft engine and helicopter transmission monitoring system models [2, 3]. In addition, analyses of testrig data for rotating machinery components have shown that, in addition to operational variations, variations introduced during design, manufacturing, and assembly significantly influence the final response characteristics of such systems [1, 3].

To address these issues more thoroughly, ongoing research at NASA Ames Research Center and at the University of Missouri-Rolla explores an empirical and simulation-based approach to help develop deterministic and probabilistic models of healthy and faulty data. The purpose is to provide enhanced signal models that will help with the roadbloacks facing anomaly detection algorithms, and hence the vehicle health monitoring systems in which they are implemented.

Long-Term Goal: Turbine Crack Damage Detection

The unexpected failure of a gas turbine can stop missions and in the worst case result in the death of crew members. Health monitoring of aircraft engines is an integral part of many maintenance plans. Accurate and reliable health monitoring can result in significant cost savings.

The design of a health monitoring system requires the careful study of potential failure modes, their effects and criticality of those effects. Banks et al. [4] review this process for the U.S. Marine Corps Advanced Amphibious Assault Vehicle (AAAV). Lifson et al. [5] analyze the practices, benefits, and limitations of several types of vibration monitoring systems used with industrial Gas Turbines. Aretakis and Mathioudakis [6] use Wavelet Analysis to detect fouled rotor blades, a twisted rotor blade, and mistuned stator vanes.

A crack in a blade rotating at high speed can devastate an engine beyond repair. An extensive post fracture failure analysis of wind tunnel compressor blade was made by Hampton and Nelson [7], and reveals much about crack initiation and growth but this is far too late for many applications. Ganesan et al. [8] use a finite element method to study the dynamic response of high speed rotors with variation in elastic modulus and mass density.

Turbine blades have complex geometries and are subject to complex excitation signals. With a long term goal to completely understand the vibrational response of healthy and damaged turbine blades subject to different excitations, we begin with the simpler problem of understanding the impact of manufacturing variations on healthy and damaged simple beams. As basic knowledge is developed, future work will explore the more complex turbine blade problem.

Related Work

A large effort has been made to explore the vibrational characteristics of damaged beams. Hu and Liang [9] use an integrated approach of a massless spring and a continuum damage concept to develop a crack detection technique. Gudmundson [10] develops models that enable the simulation of eigenfrequency changes of structures due to cracks and other geometrical changes. In Gudmundson [10] the models are benchmarked against finite element analysis and experimental results from Wetland [11]. Chondros et al. [12] develop a continuous vibration model for the lateral vibration of a cracked Euler-Bernoulli beam with open edge cracks. Chondros et al. have also explored a crack model for transverse, longitudinal, and other vibrations as well as beams with different end conditions [13–15] Mengcheng [16] and Yokoyama [17] use a theoretical line-spring model and Euler-Bernoulli beam theory to approximate the response of cracked beam vibrations. Maiti [18] develops theoretical models for the vibration characteristics of cracked beams with a linearly variable cross section (wedge shaped beams). Using experimental methods, Ju et al. [19] diagnose the fracture

damage of structures using modal frequency methods.

Though a large effort has been expended in developing models that can be used to simulate the vibrational characteristics of fractured beams, each of the models assume a beam with ideal geometry and material properties. Little work has been done to determine the combined effects of manufacturing variation and fractures on vibrational characteristics of structures.

Research Focus: Variational Failure Models

In a prior publication, the authors presented a feasibility study on the use of probabilistic methods (e.g., Monte Carlo simulation) using a simple example in design, and compared these methods to more traditional variation analysis techniques [20]. A case study was presented, focusing on the analysis of a lumped parameter dynamic model for a complex cam-follower, followed by an analysis of vibration data obtained from such a model. The Monte Carlo simulation technique was used to vary a subset of the design parameters. The effect on the vibration response was explored to determine whether probabilistic methods can be used to model the inherent variations observed in the dynamic response of complex systems [20]. Manufacturing process capability variations on as little as one of the modeling elements (e.g., the spring constant) was shown to cause significant variations in the acceleration signature of the cam-follower system.

The question that remained unanswered in the previous study was whether these variations, caused by variations in the manufacturing process, would have an impact on the monitored signature when combined with a failure signature. In this paper, this question is being explored further by using two different modeling approaches to generate the failure signatures, and exploring their variational characteristics when combined with inherent variations in the system and/or its components. Specifically, models are derived to study the combined impact of crack damage and manufacturing variation on the vibrational characteristics of simple beams. The transverse vibration and associated eigenfrequencies of the beams are considered as the candidate monitoring signature.

MODELING VIBRATION IN DAMAGED BEAMS

A critical and observable impact of fractures on beam vibrational response is the difference in the eigenfrequencies for the damaged and undamaged beam. Most theoretical models of cracked beams begin with a Euler-Bernoulli beam and develop special considerations to model crack damage. Here, the Euler-Bernoulli beam is developed with considerations for manufacturing variation. Crack models are added to the resultant model to explore the impacts of both manufacturing variation and structural damage.

Two different approaches are explored to determine whether the choice and fidelity of the models will have an impact on the detectability of the crack failure. The first approach uses separation of variables. This method enables the direct integration of the resulting ordinary differential equation and determination of different eigenfrequencies and eigenmodes. This approach uses a spring to model localized reduction in stiffness as a result of the cracked beam. The second approach uses a finite difference approach to enable the inclusion of both cracks and manufacturing variation to be considered. The crack model used with the finite difference approach is based on a localized decrease in Young's modulus. The crack model used with the finite difference approach is based on a localized decrease in the Young's modulus. Using both beam and crack models, Monte Carlo simulations are used to explore the impact of manufacturing variation on damaged and undamaged beams.

In the following sections, detailed derivations are presented for both models, followed by their application to an example problem to determine the distributional characteristics. Conclusions are presented on the choice of modeling techniques to define crack damage, and its impact on the monitored signal, followed by conclusions about the distributional characteristics of the monitored signatures when exposed to random manufacturing variations.

A Modal Analysis Approach

The first approach is to separate the resultant equation in time and space. The resulting spatial equation can be directly integrated to determine eigenfrequencies and eigenmodes for damaged and undamaged beams. This model will be compared to a complete solution developed from a finite difference technique with frequency characteristics of the beam extracted using a Fast Fourier Transform (FFT).

Developing the Variational Model Beginning with the Euler-Bernoulli Beam equation [21] we have

$$\rho A\frac{\partial^2 w}{\partial t^2}+\frac{\partial^2}{\partial x^2}\left(EI\frac{\partial^2 w}{\partial x^2}\right)=f(x,t) \tag{1}$$

Here, the fact that w is a function of both space and time has not been explicitly shown in the notation ($w(x,t)$). This is done to keep the notation compact as the derivation proceeds. Also, to allow a variational model to be developed, E, I, A, and ρ are functions of x ($E(x)$, $I(x)$, $A(x)$, and $\rho(x)$). Finding the free response, $f(x,t)=0$. Applying the chain rule and collecting terms of Eq. (1) gives

$$\begin{aligned} EI\tfrac{\partial^4 w}{\partial x^4}+\\ \left(2I\tfrac{\partial E}{\partial x}+2E\tfrac{\partial I}{\partial x}\right)\tfrac{\partial^3 w}{\partial x^3}+\\ \left(I\tfrac{\partial^2 E}{\partial x^2}+2\tfrac{\partial E}{\partial x}\tfrac{\partial I}{\partial x}+E\tfrac{\partial^2 I}{\partial x^2}\right)\tfrac{\partial^2 w}{\partial x^2}=-\rho A\tfrac{\partial^2 w}{\partial t^2}. \end{aligned} \tag{2}$$

Dividing Eq. 2 through by $\frac{1}{EI}$ and letting

$$\alpha_1 = \left(\frac{2}{E}\frac{\partial E}{\partial x} + \frac{2}{I}\frac{\partial I}{\partial x}\right), \tag{3}$$

$$\alpha_2 = \left(\frac{1}{E}\frac{\partial^2 E}{\partial x^2} + \frac{2}{EI}\frac{\partial E}{\partial x}\frac{\partial I}{\partial x} + \frac{1}{I}\frac{\partial^2 I}{\partial x^2}\right), \tag{4}$$

and

$$\alpha_3 = -\frac{\rho A}{EI} \tag{5}$$

gives Eq. (2) as

$$\frac{\partial^4 w}{\partial x^4} + \alpha_1\frac{\partial^3 w}{\partial x^3} + \alpha_2\frac{\partial^2 w}{\partial x^2} = -\alpha_3\frac{\partial^2 w}{\partial t^2}. \tag{6}$$

Note here that α_1, α_2, and α_3 are functions of x and not t. Because at each point x, the beam oscillates in time, separation of variable can be used to solve Eq. (6). Taking a solution of the form $w = XT$ where X is only a function of x and T is only a function of t Eq. (6) becomes

$$\frac{d^4X}{dx^4}T + \alpha_1\frac{d^3X}{dx^3}T + \alpha_2\frac{d^2X}{dx^2}T = -\alpha_3 X\frac{d^2T}{dt^2}. \tag{7}$$

Separating the terms dependent on only x and only t gives

$$\frac{\frac{d^4X}{dx^4} + \alpha_1\frac{d^3X}{dx^3} + \alpha_2\frac{d^2X}{dx^2}}{\alpha_3 X} = -\frac{\frac{d^2T}{dt^2}}{T} = p^2. \tag{8}$$

The solution to the time dependent term in Eq. (8) is

$$T = A\sin(pt) + B\cos(pt). \tag{9}$$

The spatially dependent term in Eq (8) becomes

$$\frac{d^4X}{dx^4} + \alpha_1\frac{d^3X}{dx^3} + \alpha_2\frac{d^2X}{dx^2} - p^2\alpha_3 X = 0. \tag{10}$$

The solution to Eq. (10) produces different eigenvalues p with corresponding eigenfunctions X. The eigenvalues of Eq. (10) give the natural frequencies or eigenfrequencies at which the beam vibrates with the corresponding mode shapes or eigenmodes of vibration, X. Equation (10) allows the impacts of spatially variable moments of inertia, area, density, and Young's modulus on natural frequency and mode shape to be explored. Equation (10) is a variational model. Next, a crack is added to the model.

Crack Model Different crack models have been proposed and explored computationally and experimentally. Here, a crack model from Chondros [12] is used. The ability of this crack model to predict changes in beam eigenfrequencies has shown good agreement with other models as well as experimental results [12].

The philosophy of the basic crack model is seen in Figure 1. Assuming that the crack is only apparent in its neighborhood, the crack is modeled as a local change in beam flexibility. The local compliance of the beam is then

$$c = \frac{6\pi\left(1-\nu^2\right)h\Phi(\frac{a}{h})}{EI}. \tag{11}$$

Here, Φ is computed from

$$\begin{aligned}\Phi = {} & 0.6272\left(\tfrac{a}{h}\right)^2 - 1.04533\left(\tfrac{a}{h}\right)^3 + 4.5948\left(\tfrac{a}{h}\right)^4 \\ & -9.9736\left(\tfrac{a}{h}\right)^5 + 20.2948\left(\tfrac{a}{h}\right)^6 - 33.0351\left(\tfrac{a}{h}\right)^7 \\ & +47.1063\left(\tfrac{a}{h}\right)^8 - 40.7556\left(\tfrac{a}{h}\right)^9 + 19.6\left(\tfrac{a}{h}\right)^{10}.\end{aligned} \tag{12}$$

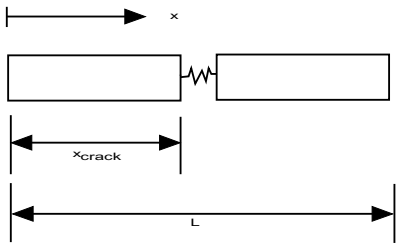

Figure 1. Crack model for the beam.

The compliance of this crack model gives boundary conditions at the location of the crack in the beam. The boundary conditions for the beam at some dimensionless crack location $\beta = x_{crack}/L$ are

$$\begin{gathered} w_l = w_r \\ \frac{\partial w_r}{\partial x} - \frac{\partial w_l}{\partial x} = EIc\frac{\partial^2 w_r}{\partial x^2} \\ \frac{\partial^2 w_l}{\partial x^2} = \frac{\partial^2 w_r}{\partial x^2} \\ \frac{\partial^3 w_l}{\partial x^3} = \frac{\partial^3 w_r}{\partial x^3}. \end{gathered} \tag{13}$$

Here, the subscripts l and r are used to denote the portions of the beam to the left and the right of the crack. Because these boundary conditions are true for all time, these boundary conditions

become

$$\begin{array}{c} X_l = X_r \\ \frac{dX_r}{dx} - \frac{dX_l}{dx} = EIc\frac{d^2X_r}{dx^2} \\ \frac{d^2X_l}{dx^2} = \frac{d^2X_r}{dx^2} \\ \frac{d^3X_l}{dx^3} = \frac{d^3X_r}{dx^3} \end{array} \tag{14}$$

as applied to the separated ordinary differential equation of Eq. (10).

Example To explore the variation model of the cracked beam developed above, a computational example is used. So that a comparison can be made to published results, the specific details of the beam are the same as those used by Hu [9].

The example beam is pinned-pinned. The transverse vibrations in the direction parallel to the beam's height (see Table 1) are those of interest for determining eigenfrequencies. The specific boundary conditions for the pinned-pinned beam are

$$\begin{array}{c} w|_{x=0} = 0 \\ \frac{\partial^2 w}{\partial x^2}|_{x=0} = 0 \\ w|_{x=L} = 0 \\ \frac{\partial^2 w}{\partial x^2}|_{x=L} = 0. \end{array} \tag{15}$$

Because these boundary conditions are true for all time, these boundary conditions become

$$\begin{array}{c} X|_{x=0} = 0 \\ \frac{d^2X}{dX^2}|_{x=0} = 0 \\ X|_{x=L} = 0 \\ \frac{d^2X}{dx^2}|_{x=L} = 0. \end{array} \tag{16}$$

and can be used with the separated ordinary differential equation of Eq. (10). The rest of the beam properties are shown in Table 1.

To simulate the manufacturing variation, only the tolerance on height and width were considered. Young's modulus, density, and Poisson's ratio are assumed to be constant. Also, the parallel edges of the rectangular cross section are assumed to remain parallel. The area and area moment of inertia are varied by allowing a variation in the height and width of the beam. The height and width tolerances are modeled as slowly varying dimensions with nominal values as in Table 1 with variation generated as a random number drawn from a normal distribution with mean 0 and standard deviation $0.00562/3m$. For each iteration in the Monte Carlo simulation, a "new" beam was generated with a different amplitude of variation. Two different cracks are explored in the example simulation. The properties of the crack are shown in Table 2. Ten thousand Monte Carlo samples were run for uncracked beams, beams with crack 1, and beams with crack 2.

Young's modulus, E	$28MPa$
density, ρ	$2350kg/m^3$
Poisson's ratio, ν	0.33
length , L	$10m$
height	$0.6 \pm 0.00562m$
width	$0.2 \pm 0.00562m$

Table 1. Physical characteristics of beam used in example simulation.

	Crack 1	Crack 2
location	$\beta = 0.25$	$\beta = 0.45$
depth	$a = 0.04783m$	$a = 0.05917m$

Table 2. Crack properties used in example simulation.

In summary, the problem is to solve Eq. (10) with boundary conditions Eq. (14) and Eq. (16) using Monte Carlo simulation to model beams of variable geometry.

Results The eigenvalue problem of Eq. (10) was solved using shooting point methods with a fitting point at the location of the crack. The specific methods used are those described by Keller [22]. The results of the simulation of various simulations are below. The basic results of beams with ideal geometry agree with the published results of Hu [9].

For the first case, a beam of ideal geometry was considered. This beam had no variation in geometry. Simulations were run to determine the first two eigenfrequencies of the undamaged beam, a beam damaged with crack 1 and a beam damaged with crack 2. The results are shown in Table 3. Compared to the undamaged beam, natural frequencies for both the first and second modes of vibration are reduced. The reduction in the first eigenfrequency is 0.18% for crack 1 and 0.53% for crack 2. The reduction in the second eigenfrequency is 0.36% for crack 1 and 0.05% for crack 2.

	undamaged beam	crack 1	crack 2
p_1	59.007	58.900	58.693
p_2	236.029	235.176	235.906

Table 3. Summary for vibrational characteristics of a beam of ideal geometry. Frequencies are listed in radians/second.

For the second case, a beam with manufacturing variations was considered. Simulations were run to determine the first two eigenfrequencies of the undamaged beam, a beam damaged with crack 1 and a beam damaged with crack 2. The results are shown in Table 4 and 5.

When comparing changes in the mean first eigenfrequency of the undamaged and damaged beam the results are the same as for a beam of ideal geometry. As with the ideal beam, the reduction in the first eigenfrequency is 0.18% for crack 1 and 0.54% for crack 2. Also note that the standard deviation is the same for the uncracked and cracked beam. The reduction in the second eigenfrequency is 0.37% for crack 1 and 0.05% for crack 2. There is some reduction in eigenfrequency standard deviation as the beams become cracked.

Histograms of the eigenfrequency distributions are shown in Figures 2 through 7. The shapes of the histograms show little change with the inclusion of manufacturing variation in the model.

	undamaged beam	crack 1	crack 2
μ_{p_1}	59.007	58.900	58.688
σ_{p_1}	0.007	0.007	0.007

Table 4. Summary of results for variational beam vibrational characteristics for the first eigenfrequency. Frequencies are listed in radians / second.

	undamaged beam	crack 1	crack 2
μ_{p_2}	236.041	235.165	235.915
σ_{p_2}	0.023	0.018	0.021

Table 5. Summary of results for variational beam vibrational characteristics for the second eigenfrequency. Frequencies are listed in radians/second.

A Finite Difference Approach

A second approach to determining the vibration characteristics of a cracked beam with manufacturing variation is developed here. This approach uses a finite difference method to produce the complete solution to the beam. Specific frequency information is extracted from a FFT of the beam signature. Also, a second approach to a crack model is used here. To model a crack, a local reduction in material stiffness is used to model the crack.

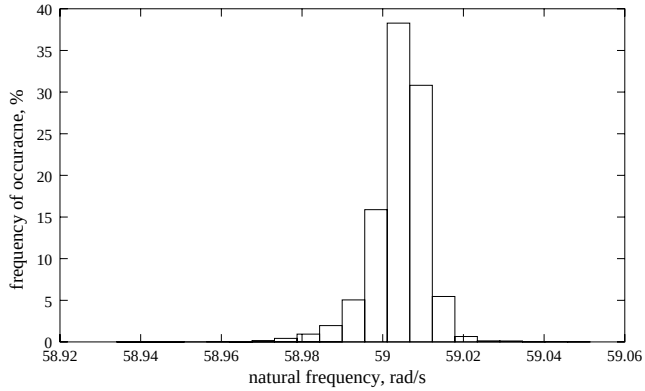

Figure 2. Histogram for the first eigenfrequency of the uncracked beam

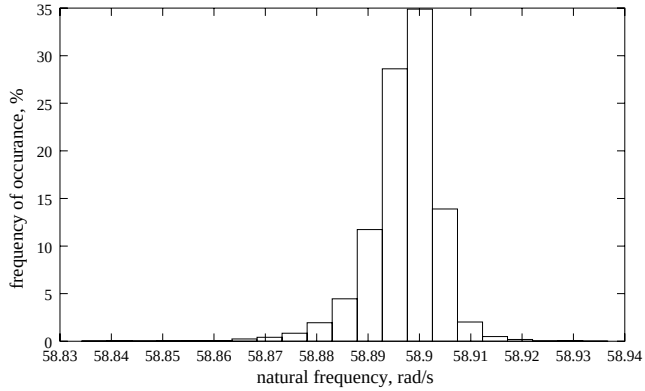

Figure 3. Histogram for the first eigenfrequency of the beam damaged with crack 1.

Problem Formulation Again, the derivation of the model begins with the Euler-Bernoulli Beam equation Eq. (1).

In the development of the finite difference equations in this section, the products ρA and EI will be kept together as a single term. Again, the explicit functional dependency of w on space and time is not shown. For a non-forced problem the external force is zero and $f(x,t) = 0$. Also, it is assumed here that ρA and EI have spatial dependency. The chain rule can be applied to give

$$\rho A \frac{\partial^2 w}{\partial t^2} + \frac{\partial^2 EI}{\partial x^2}\frac{\partial^2 w}{\partial x^2} + EI\frac{\partial^4 w}{\partial x^4} = 0. \tag{17}$$

For this solution approach, a pinned-pinned beam will be simulated. The boundary conditions for the simply supported (pinned-pinned) case for the left end are that the deflection is zero,

$$w|_{x=0} = 0, \tag{18}$$

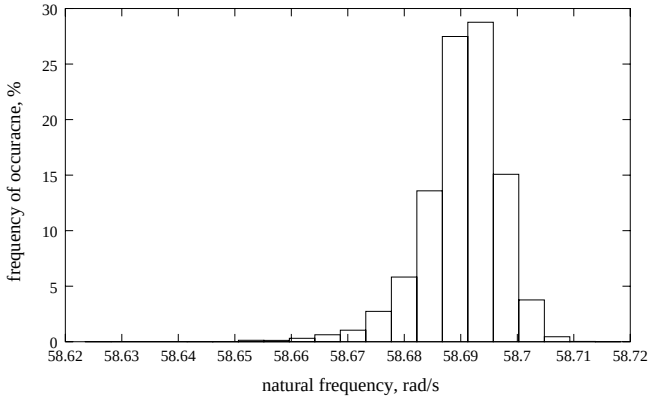

Figure 4. Histogram for the first eigenfrequency of the beam damaged with crack 2.

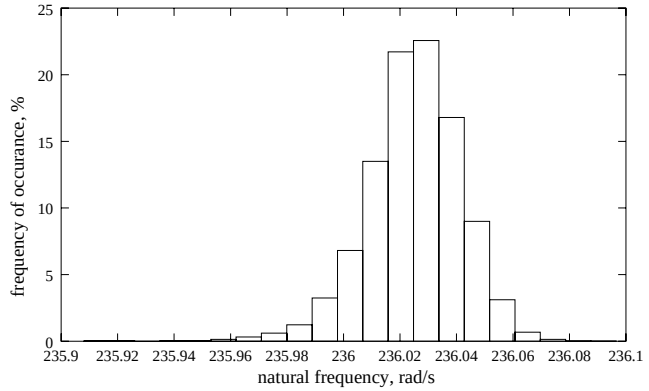

Figure 5. Histogram for the second eigenfrequency of the uncracked beam

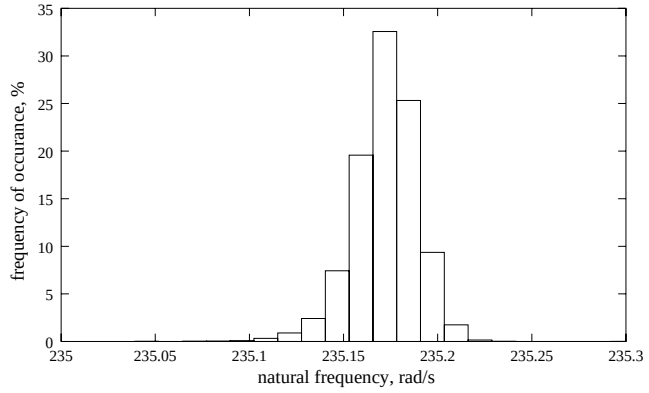

Figure 6. Histogram for the second eigenfrequency of the beam damaged with crack 1.

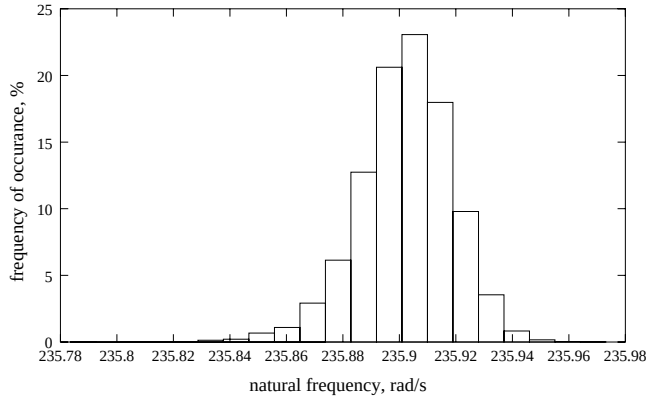

Figure 7. Histogram for the second eigenfrequency of the beam damaged with crack 2.

and that the moment is zero,

$$EI\frac{\partial^2 w}{\partial x^2}|_{x=0} = 0. \tag{19}$$

Similarly, for the right end the boundary conditions are that the deflection is zero:

$$w|_{x=L} = 0 \tag{20}$$

and the moment is zero:

$$EI\frac{\partial^2 w}{\partial x^2}|_{x=L} = 0. \tag{21}$$

The frequency behavior of damaged and undamaged beams will be extracted by applying an FFT to the complete solution of the finite difference model. To produce motion, initial conditions must be applied. The beam will be bent to an initial shape and then allowed to vibrate from the rest. This results in the following initial conditions of

$$w|_{t=0} = w_O \tag{22}$$

and

$$\frac{\partial w}{\partial t}|_{t=0} = 0 \tag{23}$$

where w_O is the initial beam shape. The problem is now fully formulated. We apply finite difference techniques in the next section.

Application of finite difference techniques To formulate algorithms for a computer program to solve, approximations for the 4th order and 2nd order terms in Eq. (17) must be substituted. The second order accurate approximation for the 4th order term from Lapidus [23] is

$$\frac{\partial^4 w}{\partial x^4} = \frac{w_{i+2,j} - 4w_{i+1,j} - 6w_{i,j} - 4w_{i+1,j} + w_{i-2,j}}{(\Delta x)^4} \tag{24}$$

where i and j are integers representing the spatial step and the time step respectively. The second order accurate approximation for the 2nd derivative of deflection with respect to x is

$$\frac{\partial^2 w}{\partial x^2} = \frac{w_{i+1,j} - 2w_{i,j} + w_{i-1,j}}{(\Delta x)^2} \tag{25}$$

Similar approximations are used for the 2nd derivative of deflection with respect to time and the 2nd derivative of EI with respect to x. The result is

$$\frac{\partial^2 w}{\partial t^2} = \frac{w_{i,j+1} - 2w_{i,j} + w_{i,j-1}}{(\Delta t)^2} \tag{26}$$

and

$$\frac{\partial^2 EI}{\partial x^2} = \frac{EI_{i+1} - 2EI_i + EI_{i-1}}{(\Delta x)^2} \tag{27}$$

Substituting Eqs. (25), (26), and (27) into Eq. (17) yields

$$\begin{aligned} &\rho A_i \frac{\left(w_{i,j+1} - 2w_{i,j} + w_{i,j-1}\right)}{(\Delta t)^2} + \\ &\left(\frac{EI_{i+1} - 2EI_i + EI_{i-1}}{(\Delta x)^2}\right)\left(\frac{w_{i+1,j} - 2w_{i,j} + w_{i-1,j}}{(\Delta x)^2}\right) + \\ &EI_i\left(\frac{w_{i+2,j} - 4w_{i+1,j} + 6w_{i,j} - 4w_{i-1,j} + w_{i-2,j}}{(\Delta x)^4}\right) = 0. \end{aligned} \tag{28}$$

Solving for the $w_{i,j+1}$ term gives

$$\begin{aligned} w_{i,j+1} = {} & 2w_{i,j} - w_{i,j-1} - \frac{(\Delta t)^2}{\rho A_i (\Delta x)^4}[\\ & (EI_{i+1} - 2EI_i + EI_{i-1})(w_{i+1,j} - 2w_{i,j} + w_{i-1,j}) \\ & + EI_i(w_{i+2,j} - 4w_{i+1,j} + 6w_{i,j} - 4w_{i-1,j} \\ & + w_{i-2,j})] \end{aligned} \tag{29}$$

Equation (29) can be used to calculate the deflection at a point on the beam at a time step, given knowledge of the deflection at that point at the two previous time steps, as well as knowledge of the deflection two spatial time steps to the left and to the right at the previous time step. This is an explicit finite difference form.

In addition to the general formulation of Eq. (29), finite difference expressions are needed for the boundary conditions and time and spatial steps where the two previous time steps are not known and the spatial steps are at the physical ends of the beam. Using a Taylor series expansion the deflection at the first time step can be represented by

$$w_{i,1} = w_{i,0} + \Delta t \frac{\partial w}{\partial t}|_{i,0} + (\Delta t)^2 \frac{1}{2} \frac{\partial^2 w}{\partial t^2}|_{i,0} \tag{30}$$

The first two terms in the right hand side of Eq. (30) are known from the initial conditions Eqs. (22) and (23). Substituting the initial conditions and solving for the 2nd derivative with respect to time gives

$$\frac{\partial^2 w}{\partial t^2}|_{i,0} = \frac{2(w_{i,j} - w_{i,0})}{(\Delta t)^2} \tag{31}$$

Substituting Eqs. (31), instead of (26) along with Eqs. (24), (25), and (27) into Eq. (17) and solving for the deflection at the first time step gives

$$\begin{aligned} w_{i,1} = {} & w_{i,0} - \tfrac{1}{2} \frac{(\Delta t)^2}{\rho A_i (\Delta x)^4}[\\ & (EI_{i+1} - 2EI_1 + EI_{i-1})(w_{i+1,0} - 2w_{i,0} + w_{i,0}) \\ & + EI_i(w_{i+2,0} - 4w_{i+1,0} + 6w_{i,0} \\ & - 4w_{i-1,0} + w_{i-2,0})] \end{aligned} \tag{32}$$

Equation 32 gives the deflection of the first time step for any point on the beam except the first and second points from the left or right where the terms $i+2$, $i+1$, $i-1$, and $i-2$ could have no meaning as those points do not exist on the beam. The boundary conditions must be used to give information about those points.

From the deflection boundary conditions (18) and (20), the deflection for the left and right ends of the beam is zero for all time steps

$$w_{1,j} = 0 \tag{33}$$

and

$$w_{n,j} = 0 \tag{34}$$

where $w_{n,j}$ represents the right end $(x = L)$ and $w_{1,j}$ represents the left end $(x = 0)$.

Next, an expression for the second point from the left and right must be found from the other two boundary conditions (19) and (21). Writing Eq. (25) for the end points (1 and n) and using the boundary conditions to set the 2nd derivative equal to zero, yields

$$EI_1\left(\frac{w_{0,j}-2w_{1,j}-w_{2,j}}{(\Delta x)^2}\right)=0 \tag{35}$$

and

$$EI_n\left(\frac{w_{I+1,j}-2w_{I,j}-w_{I-1,j}}{(\Delta x)^2}\right)=0 \tag{36}$$

Substituting the values from Eqs. (33) and (34) into those above gives

$$w_{0,j}=-w_{2,j} \tag{37}$$

and

$$w_{n+1,j}=-w_{n-1,j} \tag{38}$$

Writing Eq. (32) for the points 2 and $n-1$ and substituting into Eq. (33), (34), (37), and (38) results in expressions for these second points at the first time step:

$$\begin{aligned} w_{2,1} = w_{2,0} - \tfrac{1}{2}\tfrac{(\Delta t)^2}{\rho A_2(\Delta x)^4}[\\ EI_2(w_{4,0}-4w_{3,0}+5w_{2,0})+ \\ (EI_3-2EI_2+EI_1)(w_{3,0}-2w_{2,0})] \end{aligned} \tag{39}$$

and

$$\begin{aligned} w_{n-1,1} = w_{n-1,0} - \tfrac{1}{2}\tfrac{(\Delta t)^2}{\rho A_2(\Delta x)^4}[\\ (EI_n-2EI_{n-1}+EI_{n-2}) \\ (-2w_{n-1,0}+w_{n-2,0}) \\ +EI_{n-1}(5w_{n-1,0}-4w_{n-2,0}+w_{n-3,0})] \end{aligned} \tag{40}$$

Also, by writing Eq. (29) about the same points as above but for any time step $j+1$ yields:

$$\begin{aligned} w_{2,j+1} = 2w_{2,j} - w_{2,j-1} + \tfrac{(\Delta t)^2}{\rho A_2(\Delta x)^4}[\\ (EI_3-2EI_2+EI_1)(w_{3,j}-2w_{2,j}) \\ +EI_2(w_{4,j}-4w_{3,j}+5w_{2,j})] \end{aligned} \tag{41}$$

and

$$\begin{aligned} w_{n-1,j+1} = 2w_{n-1,j} - w_{n-1,j-1} + \tfrac{(\Delta t)^2}{\rho A_{n-1}(\Delta x)^4}[\\ (EI_n-2EI_{n-1}+EI_{n-2})(-2w_{n-1,j}+w_{n-2,j}) \\ +EI_{n-1}(5w_{n-1,j}-4w_{n-2,j}+w_{n-3,j})] \end{aligned} \tag{42}$$

Equations (22), (32), (39), (40) are used in a program to give a complete data set for the initial deflection of the beam and the deflection of the first time step. Equations (41) and (42) are then calculated for a time step, Eq. (29) is then calculated for each internal point on the beam.

Since, this is an explicit formulation the choice of step sizes must meet the following stability criterion [24]:

$$2\sqrt{\frac{EI}{\rho A}}\frac{(\Delta t)}{(\Delta x)^2}\leq 1. \tag{43}$$

Parameter variation and crack modeling The purpose of using the finite difference technique was to find solutions to Euler-Bernoulli beams with variation in the material properties and geometry. This section will consider how the variation due to manufacturing tolerances and cracks was modeled.

The McGraw-Hill Machining and Metal Working Handbook [25] gives tolerances for many manufacturing techniques and for different parts. Rarely do these tolerances exceed 1% of the nominal dimension.

This paper considers a beam with a square cross section but the base and height may differ at any point on the beam's length by $\pm 1\%$ from the nominal dimension. To generate these differences the following statement is used

$$dim = 0.9dim_n + 2\times 0.01 dim_n \times rand \tag{44}$$

The base and height were generated separately for a number of desired subdivisions of the length and then substituted into the formulas for I and A. When multiplied by modulus of elasticity and density, this results in data for the $EI(x)$ and $pA(x)$ functions.

The influence of the crack was modeled using the damage mechanics approach by DiPasquale [26]. The damage parameter is defined as

$$d=\frac{A_d}{A_T} \tag{45}$$

where $A_d = b\times a\times K$. The stress concentration factor used on A_d for an open crack was given by [27]

$$K=\sigma\sqrt{\pi a F(\lambda)} \tag{46}$$

with

$$F(\lambda) = \sqrt{\frac{2}{\pi\lambda}\tan\frac{\pi\lambda}{2}}\frac{0.923 + 0.991(1 - sin(\frac{\pi\lambda}{2}))^4}{cos(\frac{\pi\lambda}{2})} \quad (47)$$

and

$$\lambda = a/h \quad (48)$$

Using the damage parameter the stiffness degradation in the area near the crack can be calculated as

$$E = (1-d)E_0. \quad (49)$$

This degraded E is substituted into the EI formula for the node corresponding to the crack location. This incorporates the influence of the crack into the varying properties of the beam.

Example The finite difference equations and crack model developed above were used to simulate the vibrational behaviour of a cracked beam. The specific properties of the beam are shown in Table 6.

Property	Value
Length	$1m$
Nominal Base	$10cm$
Nominal Base	$10cm$
Nominal Height	$10cm$
E_0	$93750Pa$
Density	$1kg/m^3$
Crack Depth	$10mm$
Crack Location	Midpoint

Table 6. Properties of the Simulated Beam.

Results A time marching program was developed in MATLAB utilizing the equations presented above to solve the Euler-Bernoulli beam. One thousand Monte Carlo simulates were run for an uncracked beam with a randomly varying geometry the first five natural frequencies were recovered using Fast Fourier Transforms for each iteration. The Histograms for the uncracked beam are shown in Figs. 8-12.

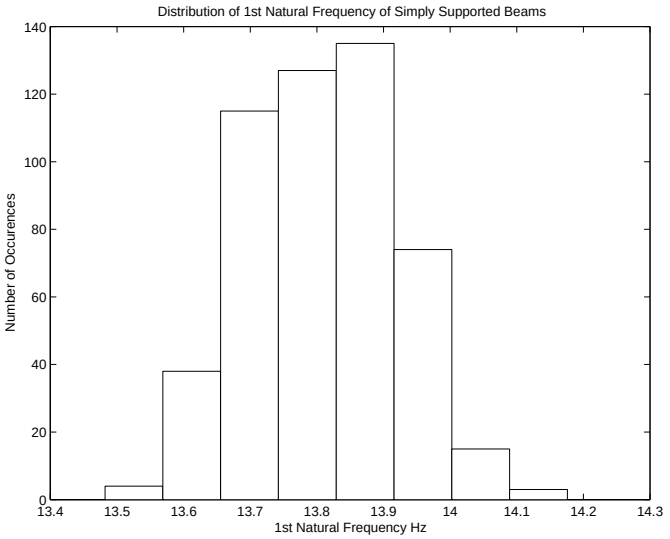

Figure 8. Histogram for the 1st natural frequency of the uncracked beam

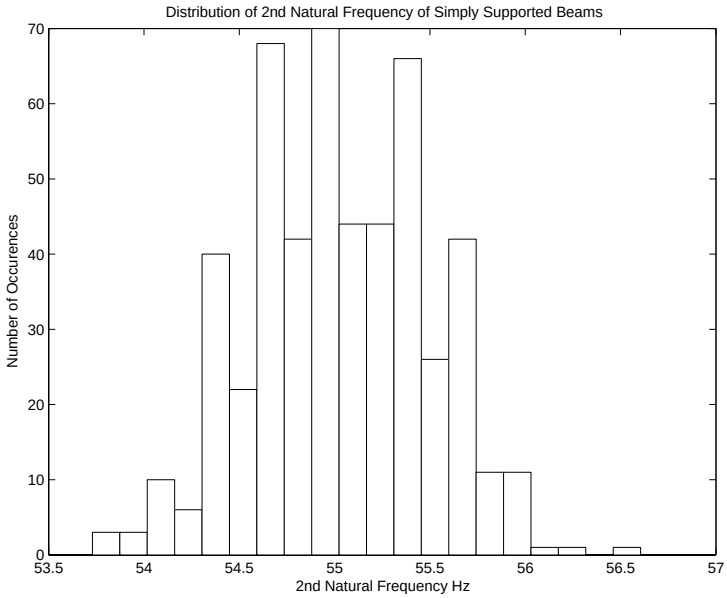

Figure 9. Histogram for the 2nd natural frequency of the uncracked beam

The program was next modified to take into account the influence of a crack at the midpoint with a depth of 10mm using the local stiffness degradation model presented above. Histograms for the first five natural frequencies are presented in Figs. 13 - 17.

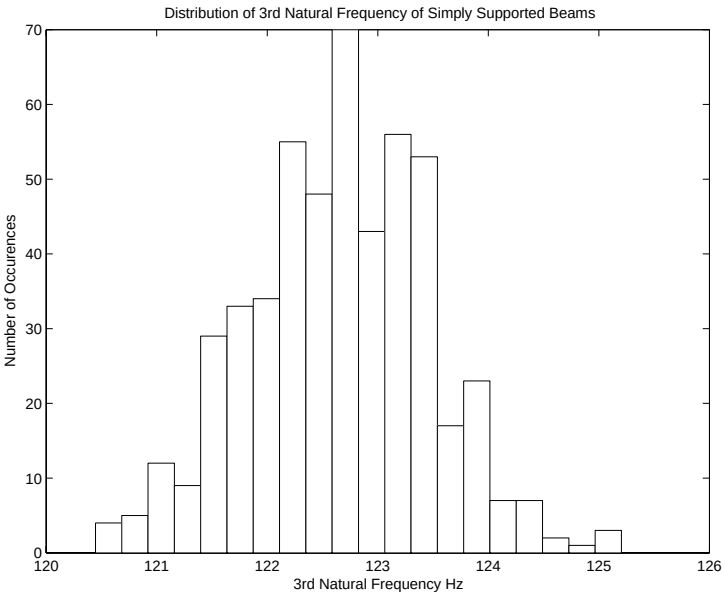

Figure 10. Histogram for the 3rd natural frequency of the uncracked beam

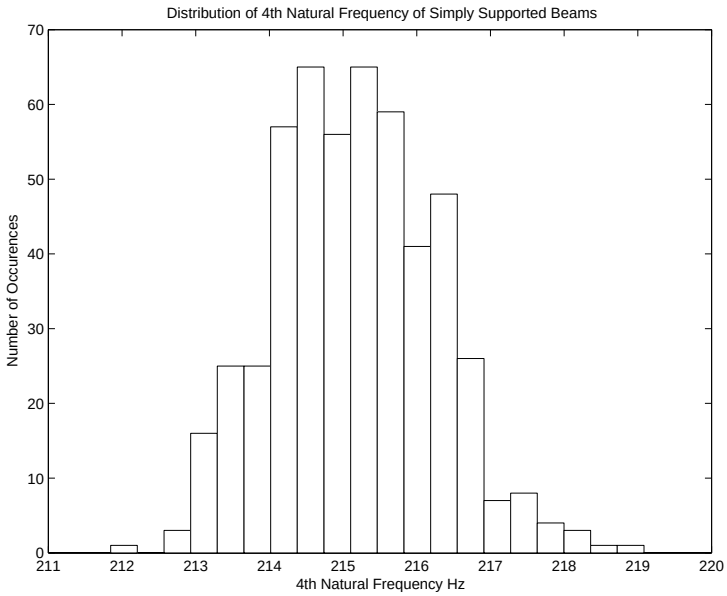

Figure 11. Histogram for the 4th natural frequency of the uncracked beam

Table 7 shows values for the mean and the standard deviation of the five recovered natural frequencies for the damaged and undamaged beams. The mean decreased as expected when the beam is cracked for the first, third, and fifth natural frequencies, but decreased for the second and fourth natural frequencies. The standard deviation increased for the first three natural frequencies but decreased for the fourth and fifth ones.

Again, the addition of manufacturing variations on the beam had little impact on the changes in natural frequency as compared to a beam of ideal geometry. Also, the standard deviations are largely the same for uncracked and cracked beams.

	Undamaged	Cracked
f_{n1} Mean	13.8072	13.7236
f_{n1} StDev	0.1285	0.1309
f_{n2} Mean	55.0465	55.1810
f_{n2} StDev	0.4475	0.5342
f_{n3} Mean	122.6632	122.1808
f_{n3} StDev	0.8146	0.8160
f_{n4} Mean	215.2019	215.4104
f_{n4} StDev	1.0989	1.0843
f_{n5} Mean	330.246	329.5359
f_{n5} StDev	1.4174	1.3948

Table 7. The Mean and Standard Deviation for the Five Natural Frequencies(fn) Recovered.

Discussion: Comparison of Modeling Approaches

Comparing the modeling approaches, both give largely the same results for the vibrational behaviour of the beam.

The separation of variables has a faster run time then the finit difference technique. Using the current algorithm, it runs about 100 times faster then the finite difference approach. The numerical algorithm used to solve the separation of variables approach has some difficulty solving for higher eigenfrequencies. This is due to the large differences in magnitude of the different derivatives. A more sophisticated algorithm can be developed to address this shortcomming. Another advantage of the separation of variables approach is that it directly solves for the mode shapes. Most solution approaches for cracked structures assume that the crack has no impact on the mode shape. Knowledge of the mode shape is used in the solution to determine crack behaviour. Exploring the impact of variation and damage on mode shapes remain future work. The model presented in this paper will adapt well to that application.

The finite difference approach has the advantage of directly providing a complete solution for w is space and time. In order to get a complete solution, the modal spatial solution of the sep-

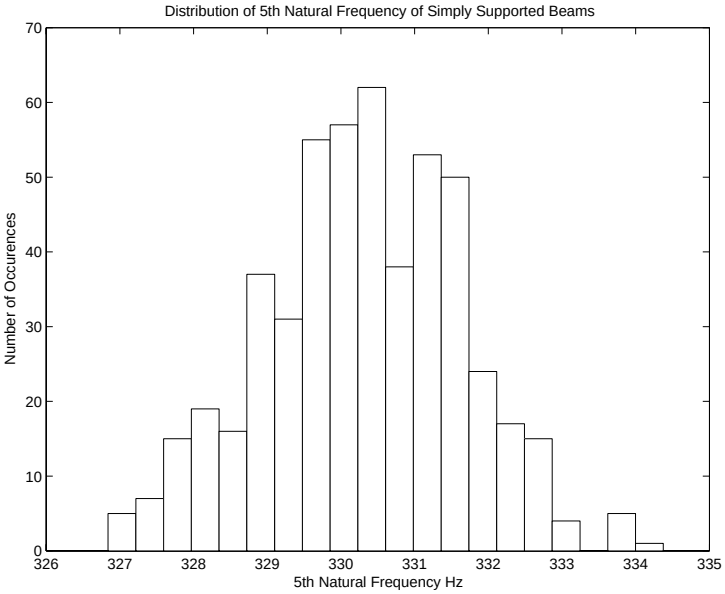

Figure 12. Histogram for the 5th natural frequency of the uncracked beam

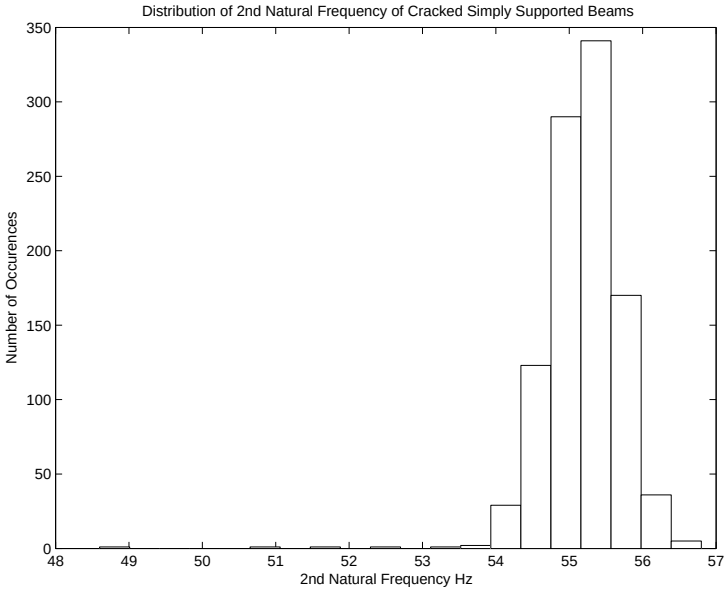

Figure 14. Histogram for the 2nd natural frequency of the cracked beam

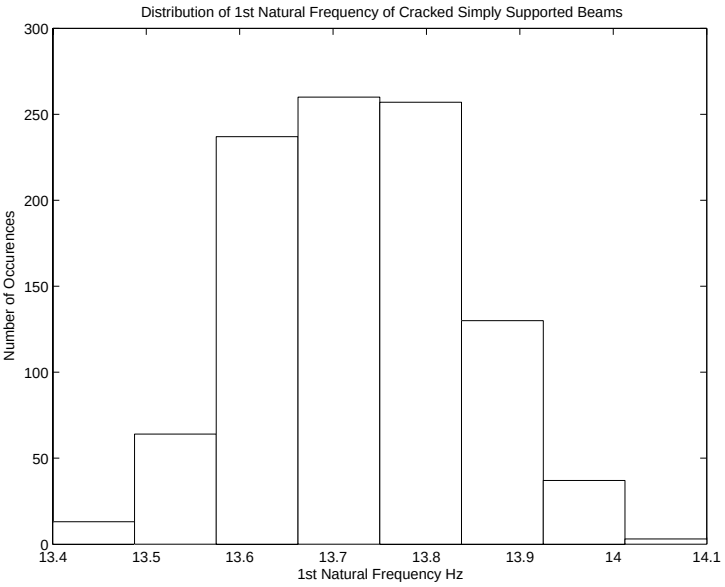

Figure 13. Histogram for the 1st natural frequency of the cracked beam

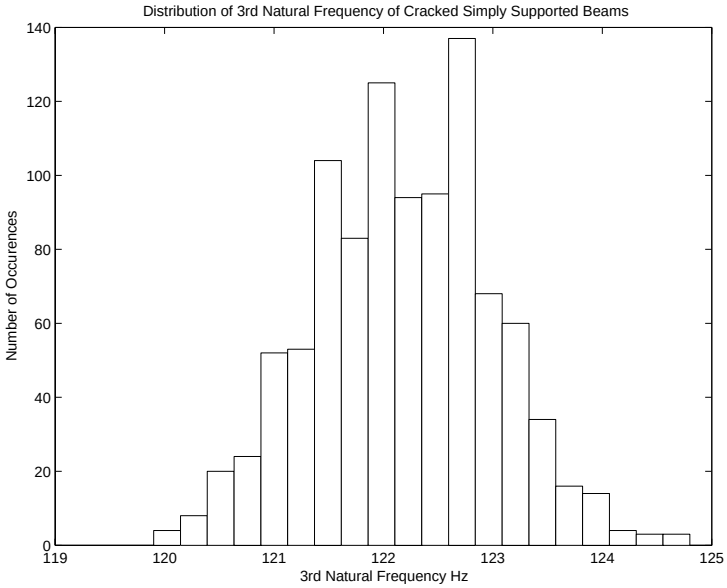

Figure 15. Histogram for the 3rd natural frequency of the cracked beam

aration of variables approach would need to be combined. The finite difference approach also has the advantage of easily solving for higher order eigenfrequencies. The problems of derivative scale associated with the separation of variables approach are not relevent to the finite difference approach.

The finite difference approach has the disadvantage that it does not directly supply frequency information. An FFT is used to extract the frequency information from the complete response. Also, determining mode shapes is difficult.

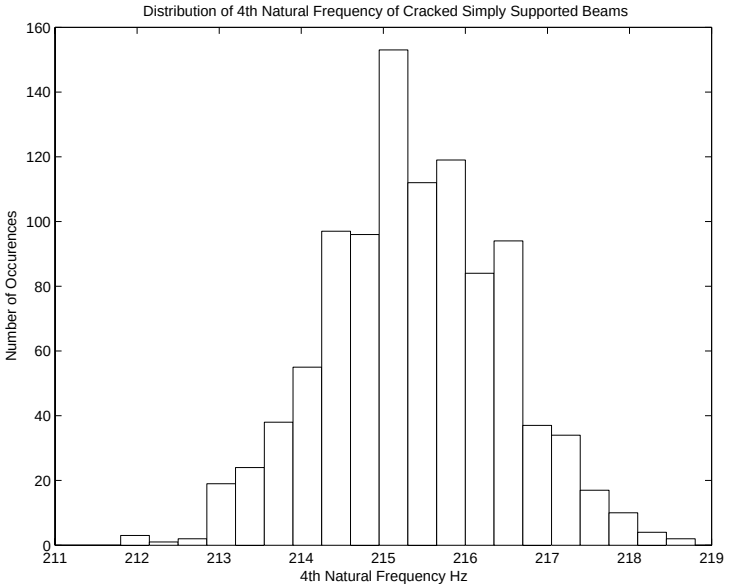

Figure 16. Histogram for the 4th natural frequency of the cracked beam

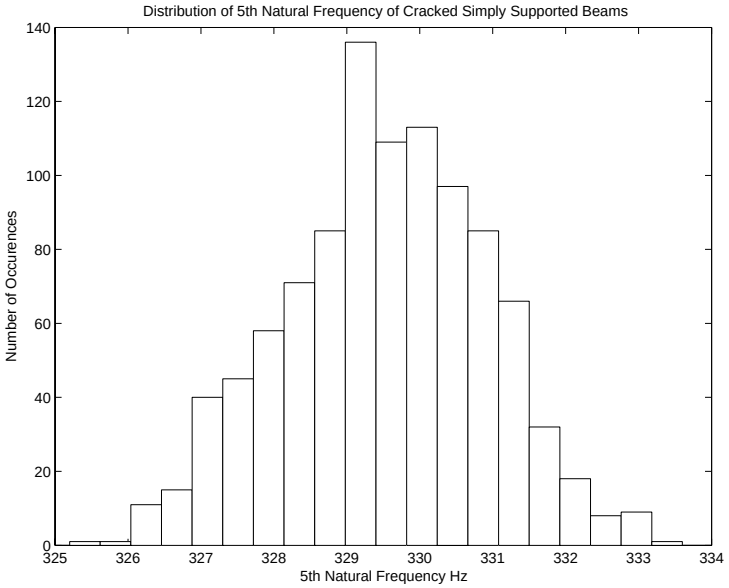

Figure 17. Histogram for the 5th natural frequency of the cracked beam

SUMMARY AND FUTURE WORK

In this article, the impact of manufacturing variations on the vibrational behaviour of healthy and damaged pinned-pinned beams was explored. These modelling methods are being developed toward a long term goal of generating a complete understanding of turbine blade behaviour with respect to health monitoring.

Two solution methodologies are employed. The first develops a variational beam model and uses separation of variables and direct integration of the spatial portion to determine the vibrational characteristics of the damaged and undamaged beam. The second uses a finite difference method to produce a complete solution to an undamaged and damaged beam. Fast Fourier Transforms are used to extract fequency information from the complete response. The two different solution methods also employed different crack models.

Both solution methods gave similar results. The inclusion of manufacturing variation on a pinned-pinned beam of the nominal characteristics simulated here has minimal impact on changes in eigenfrequencies as compared to a significant crack.

Critical future work includes validating the results of this article experimentally. With experimental validation, the models can be benchmarked and error assessed. With refined numerical solution routines that have known accuracy and resolution, more detailed models of turbine blades can be explored.

ACKNOWLEDGMENT

This research was supported by NASA grant NCC 2-5490.

REFERENCES

[1] Tumer, I., and Huff, E., 2002. "On the effects of production and maintenance variations on machinery performance". Journal of Quality in Maintenance Engineering, **8** (3), pp. 226–238.

[2] Tumer, I., and Huff, E., 2002. "Analysis of triaxial vibration data for health monitoring of helicopter gearboxes". ASME Journal of Vibration and Acoustics, **125** (1), pp. 120–128.

[3] Huff, E., Tumer, I., Barszcz, E., Dzwonczyk, M., and McNames, J., 2002. "Analysis of maneuvering effects on transmission vibrations in an AH-1 Cobra helicopter". Journal of the American Helicopter Society, **47** (1) [January], pp. 42–49.

[4] Banks, J., Reichard, K., and Brought, M., 2002. "Development of the asset health management system for the marine corps advanced amphibious assult vehicle". Proceedings of the Society for Machinery Failure Prevention Technology, **56** (2) [Apr.], pp. 277–286.

[5] Lifson, A., Quentin, G., Smalley, A., and Knauf, C., 1989. "Assessment of gas turbine vibration monitoring". Journal of Engineering for Gas Turbines and Power, **111** (2) [Apr.], pp. 257–263.

[6] Aretakis, N., and Mathioudakis, K., 1996. "Wavelet analysis for gas turbine fault diagnostics". *Transactions of the ASME*, **GT-343** [Jun], pp. 1–8.

[7] Hampton, R., and Nelson, H. G., 1986. "Failure analysis of

a large wind compressor blade". *ASTM Special Technical Publication*, **918**, pp. 153–180.

[8] Ganesan, R., Ramu, S., and Sankar, T., 1993. "Stochastic finite element analysis for high speed rotors". Journal of Vibration and Acoustics, **115** (3) [Jan.], pp. 59–64.

[9] Hu, J., and Liang, Y., 1993. "An integrated approach to detection of cracks using vibration characteristics". Journal of the Franklin Institute, **330** (5) [Sept.], pp. 841–853.

[10] Gudmundon, P., 1982. "Eigenfrequency changes of structures due to cracks, notches or other geometrical changes". Journal of the Mechanics and Physics of Solids, **30** (5) [Oct.], pp. 339–353.

[11] Wetland, D., 1972. *Aenderung der Biegeeigenfrequenzen einer idealisierten Schaufel durch Risse*. PhD thesis, University of Karlsruhe.

[12] Chondros, T. G., Dimarogonas, A. D., and Yao, J., 1998. "A continuous cracked beam vibration theory". Journal of Sound and Vibration, **215** (1) [Aug.], pp. 17–34.

[13] Chondros, T. G., and Dimarogonas, A. D., 1998. "Vibration of a cracked cantilever beam". Journal of Vibration and Acoustics-Transactions of the ASME, **120** (2) [Jul.], pp. 742–746.

[14] Chondros, T. G., Dimarogonas, A. D., and Yao, J., 1998. "Longitudinal vibration of a continuous cracked bar". Engineering Fracture Mechanics, **61** (5-6) [Dec.], pp. 593–606.

[15] Chondros, T. G., 2001. "The continuous crack flexibility model for crack identification". Fatigue and Fracture of Engineering Materials and Structures, **24** (10) [Oct.], pp. 643–650.

[16] Mengcheng, C., and Renji, T., 1997. "An approximate method of response analysis of vibrations for cracked beams". Applied Mathematics and Mechanics, **18** (3) [Mar.], pp. 221–228.

[17] Yokoyama, T., and Chen, M.-C., 1998. "Vibration analysis of edge-cracked beams using a line-spring model". Engineering Fracture Mechanics, **59** (3) [Feb.], pp. 403–409.

[18] Chaudhari, T. D., and Maiti, S. K., 1999. "Modelling of transverse vibration of beam of linearly variable depth with edge crack". Engineering Fracture Mechanics, **63** (4), pp. 425–445.

[19] Ju, F. D., and Mimovich, M. E., 1988. "Experimental diagnosis of fracture damage in structures by the modal frequency method". Journal of Vibration and Acoustics-Transactions of the ASME, **110** (4) [Oct.], pp. 456–463.

[20] McAdams, D., and Tumer, I., 2002. "Towards failure modeling in complex dynamic systems: impact of design and manufacturing variations". In ASME Design for Manufacturing Conference, vol. DETC2002/DFM-34161.

[21] Inman, D., 1976. *Engineering Vibration*. Prentice Hall, Engelwood Cliffs, NJ.

[22] Keller, H. B., 1976. *Numerical Solution of Two Point Boundary Value Problems*. Society for Industrial and Applied Mathematics, Philedelphia, Pennsylvania.

[23] Lapidus, L., and Pinder, G., 1982. *Numerical Solution of Partial differential Equations in Science and Engineering*. John Wiley and Sons, New York, NY.

[24] Bilbao, S., 2002. *Wave and Scattering Methods for the Numerical Integration of Partial Differential Equations*. PhD thesis, Stanford University.

[25] Walsh, R., 1999. *McGraw-Hill Machining and Metal Working Handbook*. McGraw-Hill, New York, NY.

[26] Dipasquale, E., Ju, J., Askar, A., , and Cakmak, A., 1990. "Relation between global damage indices and local stiffness degradation". Journal of Structural Engineering, **116** (5) [May.], pp. 1440–1456.

[27] Murphy, K., and Zhang, Y., 2000. "Vibration and stability of a cracked translating beam". Journal of Sound and Vibration, **237** (2) [Oct.], pp. 319–335.